

## Supplemental Data

### Biallelic *TBCD* Mutations Cause Early-Onset

### Neurodegenerative Encephalopathy

Noriko Miyake, Ryoko Fukai, Chihiro Ohba, Takahiro Chihara, Masayuki Miura, Hiroshi Shimizu, Akiyoshi Kakita, Eri Imagawa, Masaaki Shiina, Kazuhiro Ogata, Jiu Okuno-Yuguchi, Noboru Fueki, Yoshifumi Ogiso, Hiroshi Suzumura, Yoshiyuki Watabe, George Imataka, Huey Yin Leong, Aviva Fattal-Valevski, Uri Kramer, Satoko Miyatake, Mitsuhiro Kato, Nobuhiko Okamoto, Yoshinori Sato, Satomi Mitsuhashi, Ichizo Nishino, Naofumi Kaneko, Akira Nishiyama, Tomohiko Tamura, Takeshi Mizuguchi, Mitsuko Nakashima, Fumiaki Tanaka, Hirotomo Saito, and Naomichi Matsumoto

## **Supplemental Note: Case Reports**

### **Family 1**

Two affected individuals were born to non-consanguineous Japanese parents. Individual 1 (II-1) was born at 42 gestational weeks by vaginal delivery. Her birth weight was 2864 g [−0.68 standard deviation (SD)]. Mild hydramnion was noted during the pregnancy. Apgar scores were 1 after 1 min and 2 after 5 min. No spontaneous breathing or voluntary movements, even of the face, were observed at birth; therefore resuscitation, intubation, and mechanical ventilation were immediately started. At birth, a weak light reflex, anisocoria (right > left), marked hypotonia, paralysis of the body below the neck, and the absence of deep tendon reflex (DTR) were observed. Bone fractures of the bilateral humerus and left femur, general osteopenia, bowing of the femur and radius, and narrowing of the ribs were also noted. Serum creatine kinase (CK) was elevated at birth (1338 IU/L, normal range: 35–160 IU/L). At 1 month, the light reflex was absent. Brain computed tomography (CT) at 8 months of age showed diffuse atrophy of the cerebrum, cerebellum, brain stem, and cervical cord. Brain magnetic resonance imaging (MRI) at 2 years showed severe diffuse atrophy of the entire central nervous system (CNS) including the spinal cord. Particularly in the cerebellum, normal anatomical structure was almost absent. Muscle CT and MRI did not detect any substantial muscle volume, only soft tissue signals. Facial photographs at 3 months, and 1 year, and 3 years are shown in Figure 1D and Figure S4.

Unfortunately, brain imaging data from this individual were unavailable. Despite a tracheotomy she died of respiratory failure at 4 years of age, and an autopsy was performed.

Individual 2 (II-2) was born at 39 weeks of gestation with Apgar scores of 1 after 1 min and 4 after 5 min. His birth weight, length, and head circumference (HC) were 2867 g ( $-0.7$  SD), 48 cm ( $-0.63$  SD) and 34.5 cm ( $+0.76$  SD). Like Individual 1, no spontaneous breathing or voluntary movements, even of the face, were seen following birth. Severe hypotonia in the extremities, multiple arthrogryposis, and absence of DTR were noted. Serum CK was also elevated at birth (CK 640 IU/L with CK-MB 145 IU/L) and reached maximum CK (1345 IU/L with CK-MB 24 IU/L) at 1 day after birth, and then decreased to the normal range in 6 days (56 IU/L). A muscle biopsy at 12 days after birth revealed nonspecific myopathic changes. Mechanical ventilation was started immediately after birth and a tracheotomy was performed. Neurogenic bladder and swallowing disturbances were also noted. Brain CT at 8 months and 20 months of age showed severe cerebral atrophy and mild atrophy of medulla and midbrain (Figure 3A). Serum and urine amino acid analysis, very long chain fatty acid and urine organic acid analysis, and cerebrospinal fluid examination were all normal. This individual was unresponsive to visual evoked potential and auditory brainstem stimulation. Motor nerve conduction velocity (MCV) and sensory conduction velocity (SCV) could not be measured due to a lack of muscle potential. At 16 years of age, a brain MRI showed progressive severe atrophy of the CNS

including the brain stem (Figure 3A). At 19 years of age, his body weight, length, and HC were 150 cm ( $-3.97$  SD), 33.0 kg ( $-3.66$  SD), and 46.5 cm, respectively. He was immobile, uncommunicative, and had no visual tracking. His facial photographs at 3, 5, 10, and 15 years of age are shown in Figure 1D and Figure S4. He passed away after an anaphylactic shock reaction to egg white at 19 years of age.

## **Family 2**

Two affected individuals were born to non-consanguineous Japanese parents. They were born without asphyxia after uneventful pregnancies. The first child (II-1; Individual 3) was born at 38 gestational weeks by cesarean section for breech presentation. Her birth weight, length and HC were 3112 g ( $-0.3$  SD), 51.0 cm ( $+1.15$  SD) and 34.5 cm ( $+1.17$  SD). Her locomotive activity decreased during the month following birth. At 2 months old, she was taken to hospital because she did not cry or smile at others. A brain MRI at 3 months revealed a chronic subdural hematoma of the left brain and bilateral periventricular leukomalacia (Figure S3). A subsequent MRI at 7 months of age showed that the brain atrophy was progressive (Figure 3B). At 5 months, hypsarrhythmia detected by electroencephalogram (EEG) led to the diagnosis of West syndrome. Vitamin B6, nitrazepam, and zonisamide treatments were ineffective. At 6 months old, she was admitted to hospital for adrenocorticotrophic hormone treatment, which was barely able to

improve her voluntary movement, vocalization, and EEG findings (decreased frequency of seizures by more than half and a disappearance of hypsarrhythmia and suppression-burst patterns), but paroxysmal activity still remained. Head control, visual tracking and eye contact were absent. Her facial expression was impassive and her eyes were directed to the left. As she was unable to cry when hungry, breast milk was fed at fixed intervals. Her eyelash, corneal, and cough reflexes were normal. Her upper limbs were tonic and the DTR of her extremities was increased. Her muscle tone was deteriorating and her muscles were becoming small and soft. Because of respiratory failure, mechanical ventilation was started at 9 months of age, and a tracheotomy was performed at 18 months. Her motor developmental delay became more evident as time progressed. Facial photographs at 4 months and 1 year 10 months are shown in Figure 1D and Figure S4. At 2 years, she lost DTR and had tongue fasciculation, which may indicate the disease is affecting the lower motor neurons. At 4 years of age, brain CT indicated marked atrophy of the CNS with ventricular enlargement (Figure 3B and 3C). At the age of 11 months, MCV (right median nerve: 27 m/sec, left median nerve: 31 m/sec, normal range:  $42.3 \pm 6.4$  m/sec) was delayed and SCV (between the index finger and the wrist) (right median nerve: 34 m/sec, left median nerve: 36 m/sec, normal range:  $32.6 \pm 6.4$  m/sec) was normal, and visual evoked potential was undetectable. At least four episodes of elevated CK were noticed (285 IU/L at 7 months, 249 IU/L at 8 months, 199 IU/L at 13 months, and 182 IU/L at 3 years, normal range:

41–153 IU/L). These elevations may be explained by frequent tonic seizures. Currently, she is 10 years old and immobile.

The second child (II-2; Individual 4), a 7-year-old boy, was born at 39 weeks gestation by vaginal delivery. His birth weight, length, and HC were 3548 g (+1.36 SD), 51.5 cm (+1.2 SD) and 34.0 cm (+0.38 SD), respectively. He was hypotonic at 1 month of age. He was brought to hospital at 4 months with absent head movement, absent visual tracking and muscle weakness was noted. At 5 months of age, his locomotor activity, vocalization, and crying were weak and he made no eye contact. An ophthalmological examination revealed bilateral optic nerve atrophy, but no other fundus abnormalities. Routine laboratory tests were within normal ranges except for the slight elevation of serum aspartate aminotransferase (57 IU/L), alanine aminotransferase (65 IU/L), and CK (528 IU/L). After that, elevated CK was also observed at least three times: 752 IU/L at 11 months IU/L, 279 IU/L at 14 months, and 177 IU/L at 16 months. EEG showed multiple spikes in the occipital lobes (right > left). MCV (right median nerve: 20 m/sec, normal range: 37.0±4.4 m/sec, right ulnar nerve: 28 m/sec, normal range: 40.5±4.2 m/sec) was decreased and SCV (between the index finger and the elbow) (right median nerve: 42 m/sec, normal range: 38.4±5.4 m/sec, right ulnar nerve: 44 m/sec, normal range: 44.1±4.1 m/sec) was normal at 5 months of age. Brain MRI at 5 months and CT scans at 1 year and 6 months and 2 years showed progressive diffuse cerebral atrophy predominantly in the frontal lobe (enlargement of the

subdural space and lateral ventricles and decreased volume of the white matter and prominent gyrus) and the brain stem (Figure 3D). Furthermore, brain MRI showed chronic subdural hematoma in the right lobe and cerebral atrophy mainly in the frontal lobe (Figure 3E). Low intensity of the pyramidal tract on T2-weight images suggested hypomyelination (Figure 3D). At 6 months, he suffered acute respiratory failure and was intubated and mechanically ventilated. One month later, a tracheotomy was performed. Facial photographs at 3 months, 7 months, and 1 year 5 months are shown in Figure 1D and Figure S4. A whole body CT at 6 months indicated remarkable muscle thinning and prominent fat tissues in the extremities, neck, chest, and pelvic area.

### **Family 3**

Individual 5 (II-1) and 6 (II-2) were born to non-consanguineous Malaysian Chinese parents after an uneventful pregnancy. Individual 5 was born at term via caesarian section for meconium-stained amniotic fluid. His birth weight, length, and HC were 3400 g (50<sup>th</sup> centile) and 54 cm (90<sup>th</sup> centile) and 35 cm (50<sup>th</sup> centile). No obvious dysmorphic features were noted (Facial photographs at 1 and 2 years of age are shown in Figure 1D and Figure S4). Until 4 months of age, his development was almost normal regarding muscle tonus, cooing, and smiling in response to others, but after that his development was delayed and accompanied by poor head

control and hypotonia. At 6 months of age, he had frequent and refractory generalized tonic seizures that were partially controlled by sodium valproate and clonazepam. A ketogenic diet started from 6 months of age was effective, but he showed progressive neuroregression. During his last examination at 2 years of age, he had severe microcephaly (HC 44 cm,  $-5$  SD) and profound psychomotor retardation with generalized hypotonia, marked head lag, hyperreflexia, and positive plantar reflex. He was almost immobile and unable to roll over or grasp objects. He was unresponsive to his surroundings, not focusing or vocalizing. Funduscopy showed bilateral pale optic discs. EEG revealed multifocal epileptiform discharges. A brain MRI at 1.5 years of age showed hypoplasia of the corpus callosum, delayed myelination, and bilateral widened subarachnoid spaces (images unavailable). He had swallowing difficulties and passed away at 4 years of age due to severe pneumonia.

His younger sister (Individual 6), a 4-year-old girl, was born after 38 gestational weeks by emergency caesarian section for fetal distress, but without neonatal asphyxia. Her birth weight, length, and HC were 3.4 kg (50<sup>th</sup> centile) and 54 cm (90<sup>th</sup> centile) and 34 cm (25<sup>th</sup> centile), respectively. Like her brother she developed normally until 4 months old. Subsequently, she became floppy and achieved no further developmental milestones, including head control. At 12 months, intractable generalized tonic seizures were seen daily with subsequent neurological regression. Her first two seizures were provoked by fever. A ketogenic diet was started but did

not achieve adequate ketosis, so was terminated. Only sodium valproate could partially control the seizures. On her last examination at 2 years 10 months of age, her weight, length, and HC were 10.6 kg (−1.5 SD), 87 cm (−1.2 SD), and 42.5 cm (−6 SD), respectively. Subtle dysmorphism was noted with a low anterior hairline, upslanted palpebral fissures and microcephaly (Figure 1D and Figure S4). She became immobile and unresponsive to her surroundings with generalized hypotonia, hyporeflexia, and marked head lag. Involuntary movement was not observed. An EEG at 1 year 4 months of age showed no epileptic discharge with normal background. A brain MRI at the same age indicated corpus callosum hypoplasia and generalized reduced white matter (Figure 3F).

#### **Family 4**

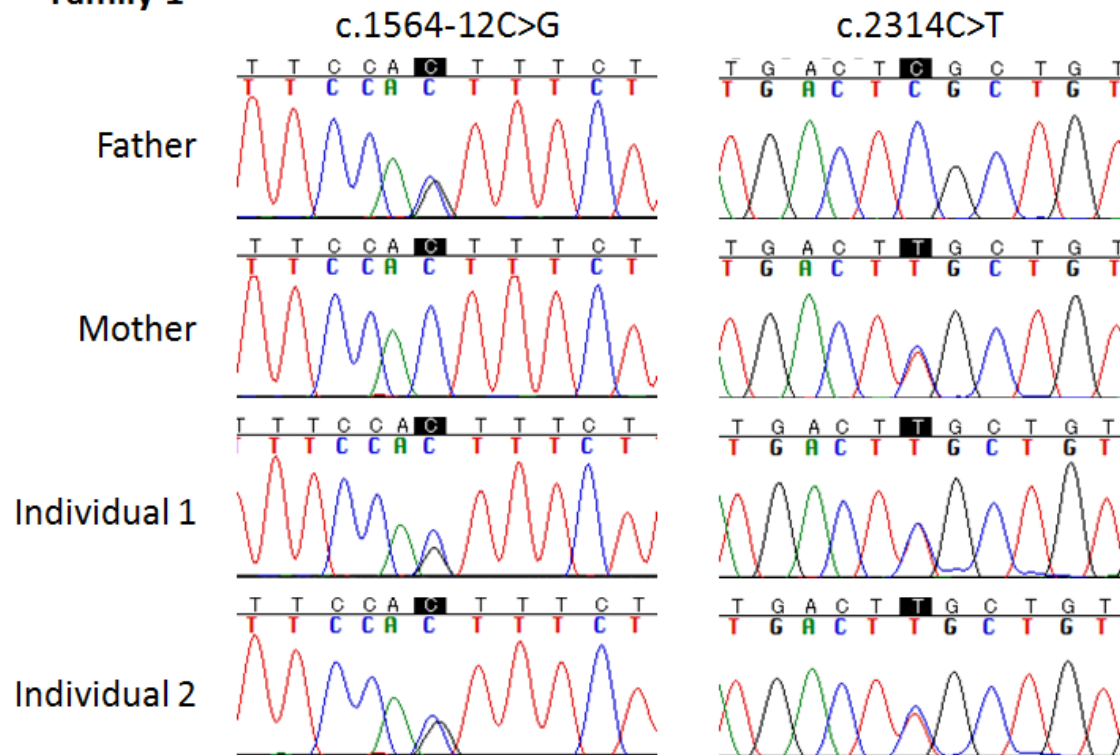
Individuals 7 (II-1) and 8 (II-2) were born to healthy first-degree cousins of Iraqi-Jewish ancestry. Individual 7 (II-1), an 18-year-old female, was born after an uneventful pregnancy. She started having febrile seizures at the age of 11 months. Later on, she developed absence seizures hundreds of times a day. Between 7–11 years of age, she was seizure-free. At 11 years, she was hospitalized for status epilepticus and intractable seizures. Currently, she has several types of seizures; complex partial, generalized tonic, and generalized tonic clonic seizures approximately twice a week. She has no myoclonic seizures. EEG revealed frequent spikes and irregular spike

wave activity (about 3 per second) with frontal predominance, but no myoclonic patterns. Brain MRI at 1.5 years revealed delayed myelination (data not shown). Visual evoked potential and electromyogram were normal. Metabolic workup including amino acids, ammonia, lactic acid, biotinidase, very long chain fatty acid and carnitine was normal. Palmitoyl-protein thioesterase and tripeptidyl-peptidase I results for neuronal ceroid lipofuscinosis were also normal. Genetic tests for Angelman and velocardiofacial syndrome were negative. She was treated with valproic acid, clonazepam, ethosuximide, lamotrigine, clobazam, topiramate, and zonisamide with no response. She also failed to respond to a ketogenic diet. Currently she is treated with levetiracetam and clonazepam to control seizures. She has severe behavioral problems such as hyperactivity and agitation, which are treated with risperidone. She started to walk unassisted at 2 years and 4 months of age. Throughout her development, she only spoke a few words, and regression occurred after the onset of seizures (11 months of age). Her current weight, height, and HC are 50 kg, 160 cm, and 51.5 cm, respectively. She is able to communicate with family members using vocal sounds. She can walk and eat independently, but needs assistance dressing. She has no sphincter control and requires diapers. She frequently drools and is classified as having moderate intellectual disability. Neurological examinations show normal eye movements, normal muscle strength, but increased muscle tone and DTR with clonus and spread of reflexes and bilateral flexor plantar response. Cerebellar functions are normal.

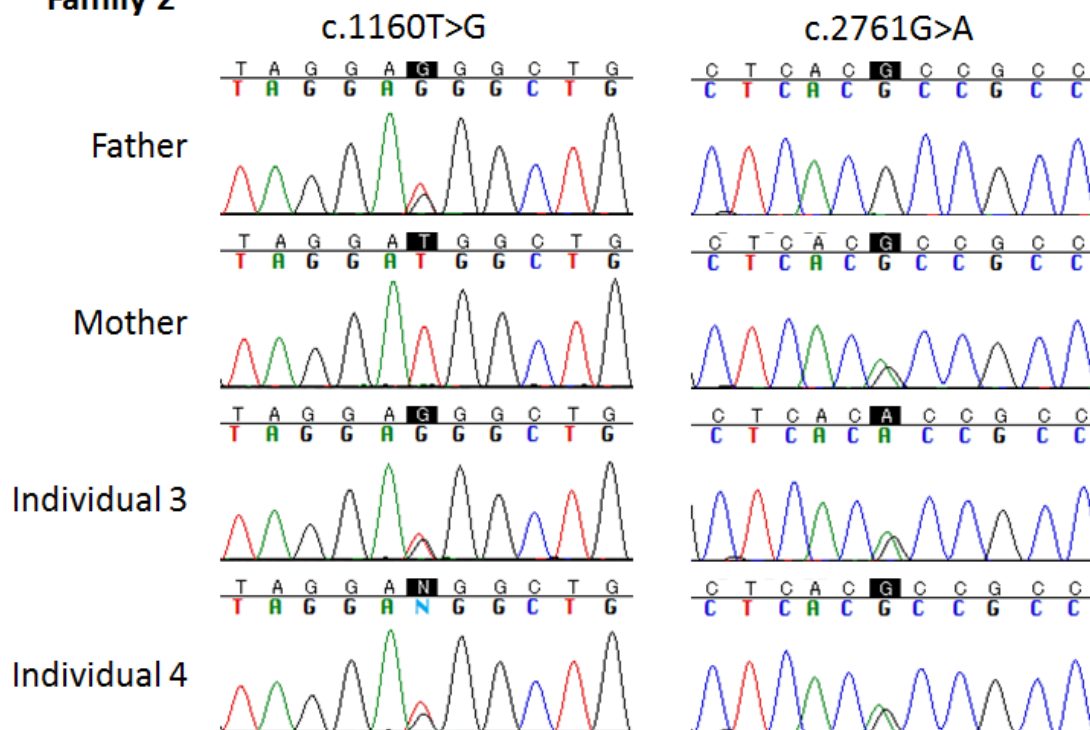
Individual 8 (II-2), a 17-year-old female, started having seizures at the age of 9 months. Currently, she has two types of seizures: generalized tonic-clonic seizures twice a week, and absence seizures with eye blinking dozens of times a day, sometimes prolonged up to 20 minutes. She does not have myoclonic seizures. A brain MRI has not been performed. She was treated with valproic acid, carbamazepine, ethosuximide, lamotrigine, levetiracetam, and topiramate, but with no response. At present, she is treated with gabapentin and sulthiame, in addition to clonazepam during attacks. She has severe behavioral problems including hyperactivity and agitation (shouting and speaking loudly), which are treated with risperidone. She only speaks a few words, but can communicate with family members using vocal sounds. She can walk independently and is able to eat unassisted, but she needs help dressing. She has sphincter control. Her cognitive level has been defined as 'moderate intellectual disability'. Her current weight, height, and HC are 50 kg, 163 cm, and 51 cm, respectively. She has 2 café au-lait spots on her skin, one of which is very large (15 cm in size) on the leg. She has no dysmorphic features. A neurological examination revealed normal eye movements, normal cranial nerves, normal muscle strength and tone, increased DTR with clonus and spread of reflexes and bilateral flexor plantar response. Cerebellar functions are normal.

## Supplementary Figures

### Family 1



### Family 2



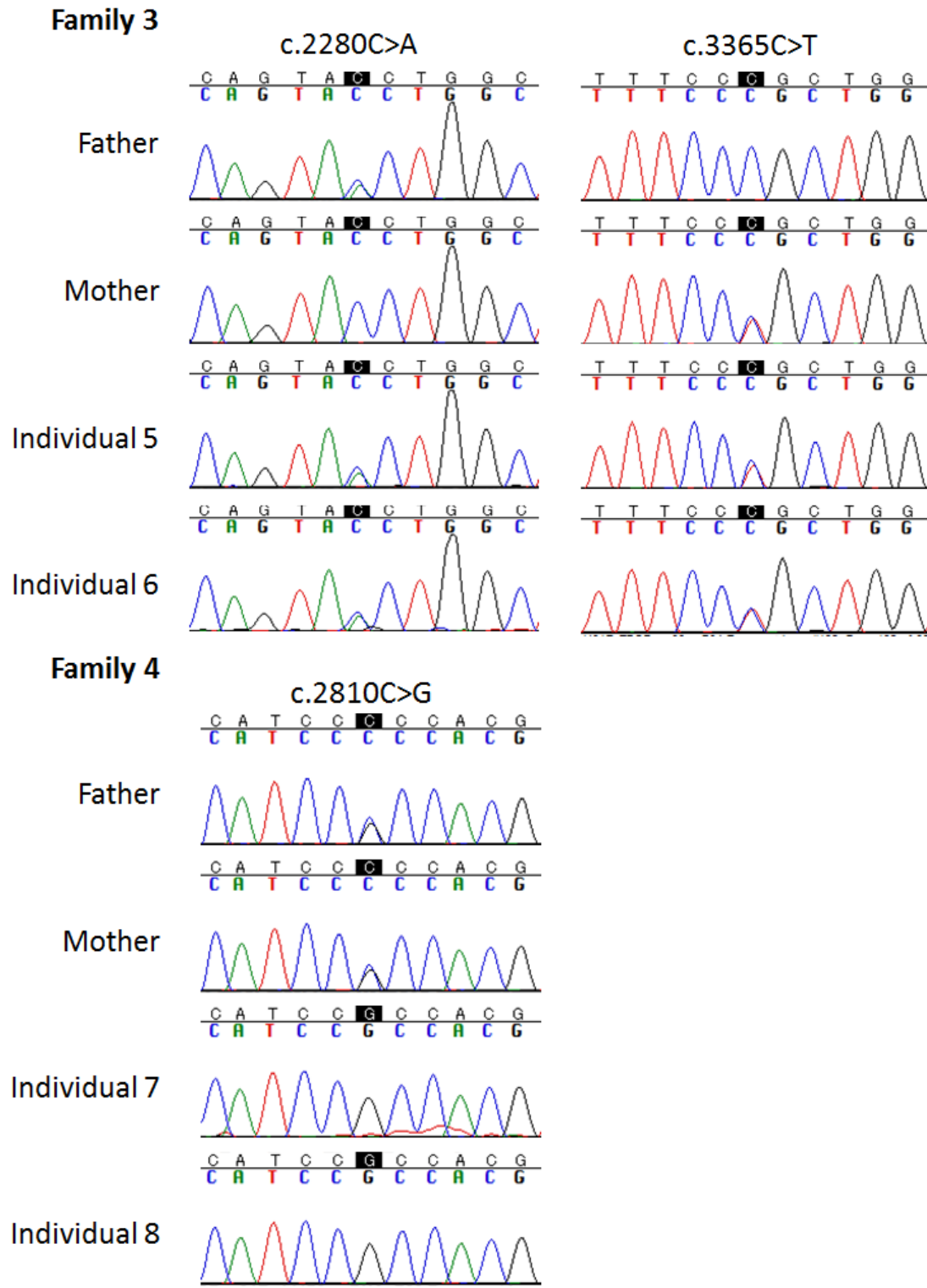


**Figure S1. Electropherograms of *TBCD* Mutations Found in Families with Early-Onset Progressive Systemic Neurodegeneration**

Affected individuals with biallelic *TBCD* mutations and their heterozygous carrier parents are clearly displayed with electropherograms.

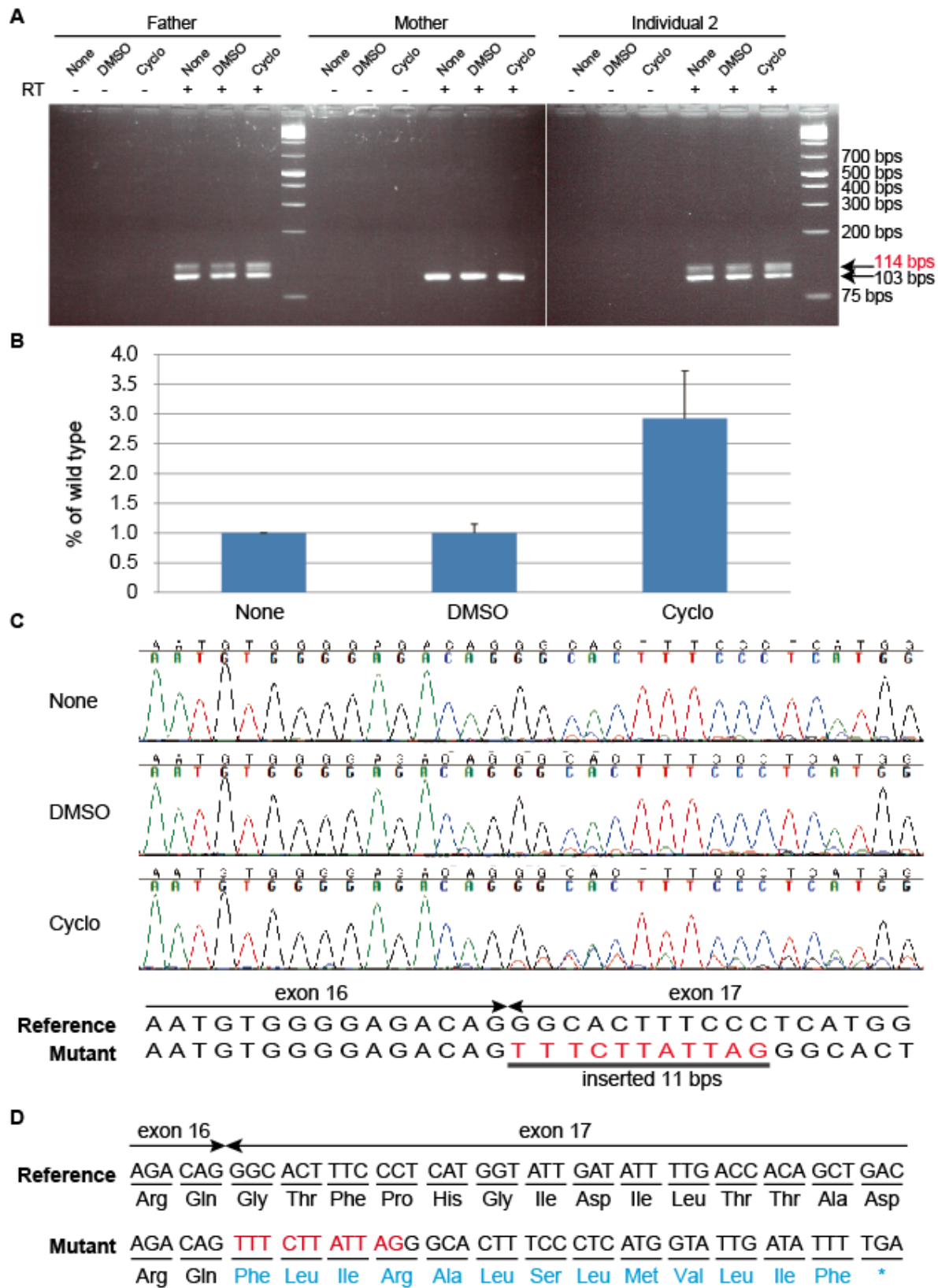
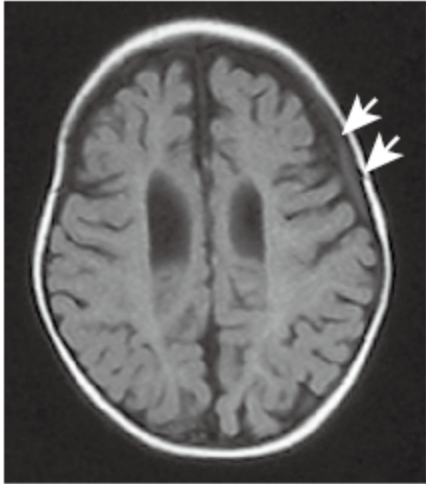


Figure S2. Aberrant Splicing Caused by c.1564-12C>G

(A) RT-PCR amplification of exon 15/16 to exon 17 using cDNA extracted from LCLs of Individual 2 and his parents using RNeasy Plus Mini Kit (Qiagen, Hilden, Germany) with/without cycloheximide to inhibit nonsense mediated decay. Total RNA was reverse-transcribed with SuperScript III First-Strand Synthesis System (Thermo Fisher, Scientific, Waltham, MA). The 103-bp product from normal allele and 114-bp aberrant product from mutant allele (c.1564-12C>G) are seen and were confirmed by Sanger method. The father and Individual 2 carrying this mutation showed the upper 114-bp product with stronger band intensity under the condition of cycloheximide. None: no treatment, DMSO: dimethyl sulfoxide, Cyclo: adding cycloheximide (Cyclo), -: with no reverse transcriptase, +: with reverse transcriptase. (B) Quantitative analysis of the aberrant band (114 bp) comparing the normal band (103 bp) under the condition of no treatment, adding solvent (control) or cycloheximide (n = 3). The gel images were captured by ChemiDoc Touch Imaging system (Bio-Rad Laboratories, Hercules, CA) and signal intensities were analyzed by Image Lab (Bio-Rad). The ratios of aberrant band to normal band were normalized to the condition of no treatment. The bar represents the standard error of the mean. (C) Electropherograms of RT-PCR products amplified from exon junction 13/14 to exon junction 18/19 (435 bps) using cDNA derived from Individual 2. Eleven nucleotides from intron 16 (in red) were aberrantly incorporated into cDNA in Individual 2 by abnormal splicing. Peak height of the abnormal allele was higher when

cycloheximide interfered with nonsense mediated mRNA decay (NMD) compared with no treatment (None) or DMSO (solvent without cycloheximide). (D) Sequence of mutant cDNA and predicted protein caused by c.1564-12C>G. The inserted nucleotides are shown in red and altered amino acids are in light blue. This splice site mutation results in a frameshift (p.Gly522Phefs\*14), but the truncated protein may not be present due to NMD. Primer sequences are available on request. The amplicon was sequenced on a 3130xl or 3500xL Genetic Analyzer (Applied Biosystems, Foster City, CA) and analyzed with Sequencher (Gene Codes, Ann Arbor, MI).



**Figure S3. Brain Image of Individual 3**

Brain MRI at 3 months indicated chronic subdural hematoma of the left brain (white arrows) and bilateral periventricular leukomalacia.

Individual 1



Individual 2



Individual 3



Individual 4



Individual 5



Individual 6



Figure S4. Facial Photographs of Affected Individuals with *TBCD* Mutations

Facial photographs of six affected individuals at different ages are shown.

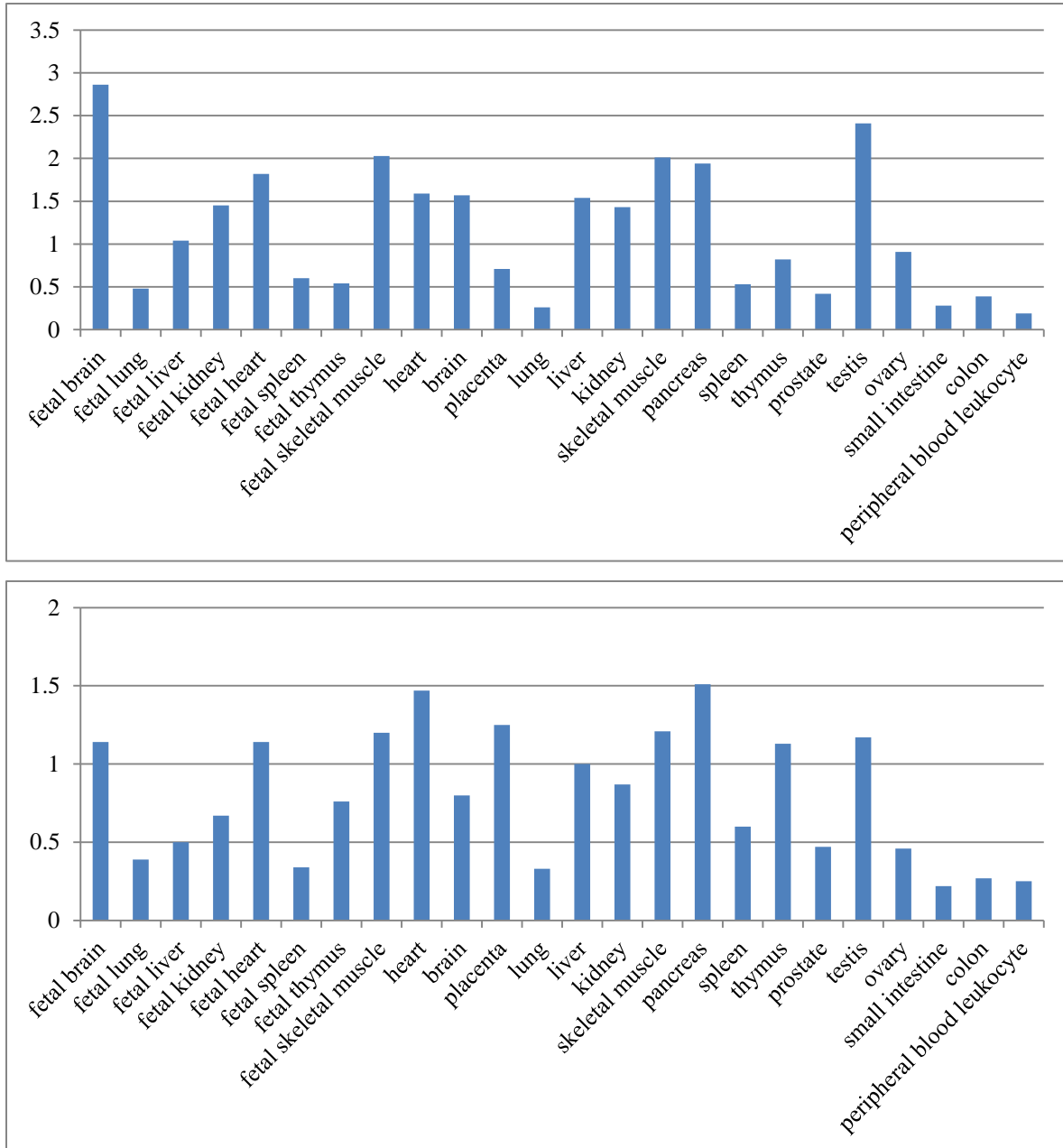


**Figure S5. TBCD Expression in Human Tissues**

Two independent experiments using two different probes (upper: Hs00195603\_m1, lower: Hs00384759\_m1) were performed after standardization to  $\beta$ -actin. cDNA from human fetal and adult tissues was purchased from Clontech (Mountain View, CA). Quantitative PCR was

performed using a Rotor-Gene Q (Qiagen) and analyzed by the Delta Delta Ct method using Rotor-Gene 6000 Series software (Qiagen). The mean of two experiments are indicated. TBCD expression is abundant in brain, heart, skeletal muscle, and testis at fetal and adult stages.

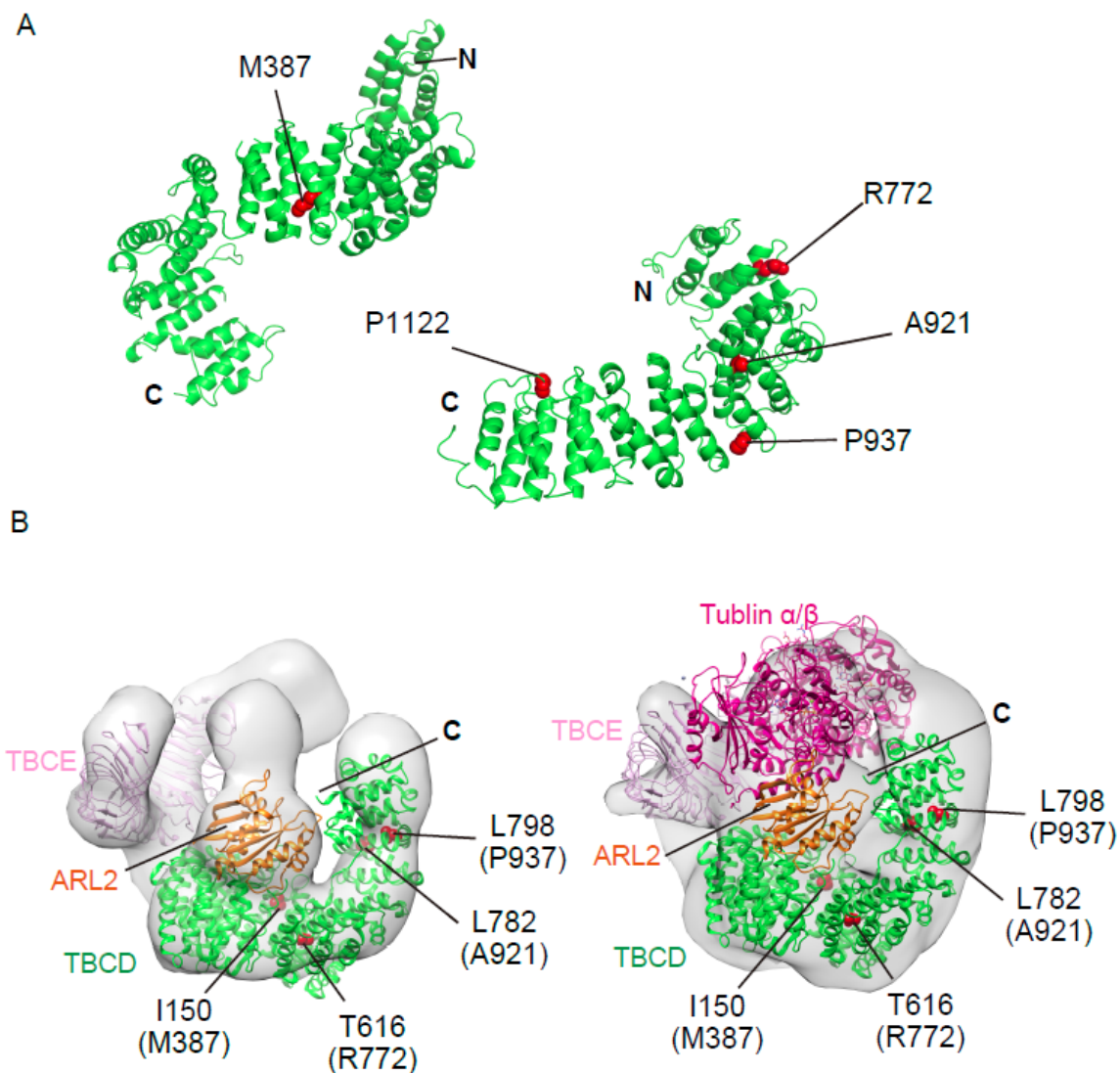


**Figure S6. Mapping of the Mutation Sites onto Homology-Modeled Structures of TBCD**

(A) The sites of the point mutations are shown in homology-modeled structures of two regions of TBCD, amino acid residues 20–695 (left) and 696–1192 (right). The residues at the mutation sites are shown as red van der Waals spheres. Annotations: N and C denote the N and C termini of the models, respectively. The models were constructed by the Phyre2 server<sup>1</sup> with each of the regions (amino acid residues 20–695 and 696–1192) as a query sequence. The crystal structure

of karyopherin Kap121p (PDB code; 3W3Z)<sup>2</sup>, which has a HEAT repeat, was selected as a structural template to build homology models of the two regions of TBCD. We verified the obtained alpha solenoid structure models using Alpha-rod Repeat Detector 2 (ARD2)<sup>3</sup> with the whole primary sequence of TBCD. (B) the EM-based pseudo-atomic models of core tubulin chaperones consisting of yeast TBCD, TBCE, and ARL2 with (right) or without (left) the yeast tubulin  $\alpha/\beta$  dimer<sup>4</sup>. The residues at the mutation sites are shown as red van der Waals spheres. Amino acid numbers for yeast Cse1 are shown with those corresponding to human TBCD in parentheses. The pseudo-atomic models were constructed according to the previous report.<sup>4</sup> Briefly, we docked the atomic models corresponding to TBCD, TBCE, and ARL2 sequentially with or without a tubulin  $\alpha/\beta$  dimer in this order into the EM maps, EMD-6390 or EMD-6392, respectively, using the ‘fitmap’ command in the UCSF Chimera software.<sup>5</sup> The following atomic models were used: the crystal structure of yeast nuclear export receptor Cse1 (PDB code 1Z3H)<sup>6</sup> for TBCD, the crystal structure of human ARL2 (PDB code 1KSJ)<sup>7</sup> for the ARL2 pillar region, and the electron crystallographic structure of  $\alpha$ - $\beta$  tubulin (PDB code 1JFF)<sup>8</sup> for the tubulin  $\alpha/\beta$  dimer. For TBCE, we constructed a homology model using the ‘intensive mode’ of Phyre2 with the human TBCE amino acid sequence as a query. The mutation positions were mapped onto the Cse1 structure as follows. We searched homologous structures for human TBCD and yeast Cse1 using Phyre2 and identified the yeast karyopherin Kap121p structure (PDB code 3W3Z)<sup>2</sup> as a

common homology model. We then mapped the mutation positions of human TBCD onto the yeast Kap121p structure, and subsequently onto the yeast Cse1 structure. The position of the P1122L mutation could not be determined because the C-terminal part of TBCE is missing from the modeled Cse1 structure. Note: The resolutions of currently available EM maps are too low to discuss the specific effects of the mutations on tubulin chaperone assembly.

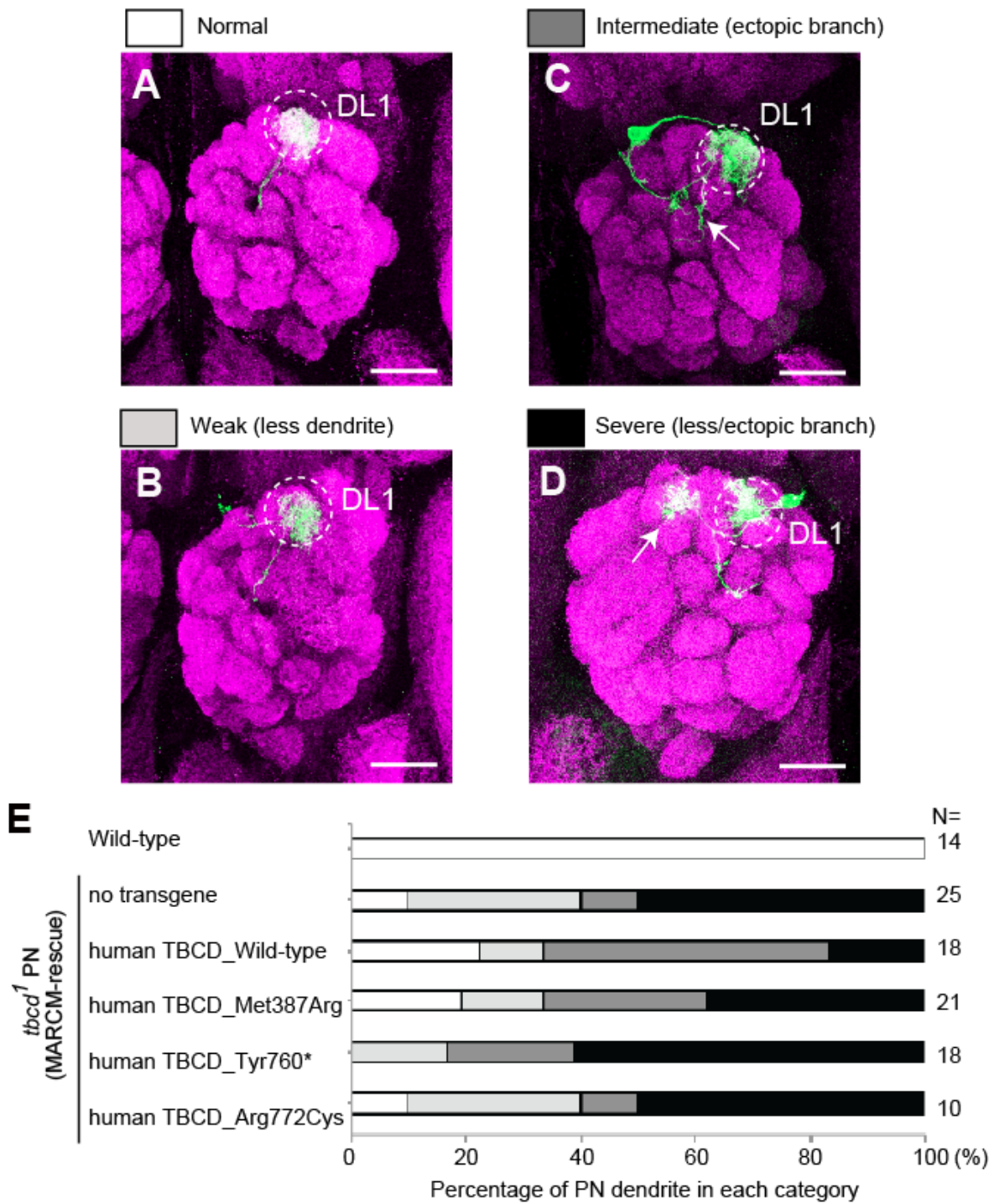


**Figure S7. Effects of Mutations on Dendrite Morphology in *Drosophila Melanogaster***

**Olfactory Projection Neurons.**

(A–D) Representative dendrite morphologies of *Drosophila* olfactory projection neurons. Dendrites of wild type DL1 single-cell clones (A) target the DL1 glomerulus. Dendrites of *tbcd*<sup>1</sup> DL1 PN exhibited arborization and branching defects as shown in B–D. Arrows in C and D indicate ectopic dendritic branches. PN morphologies and Bruchpilot (presynaptic marker) are shown in green (anti-CD8 antibody) and magenta (nc82), respectively. Scale bars: 25µm. (E) Quantification of MARCM-rescue experiments. Each gray scale corresponds to a color in A–D above. N indicates the number of MARCM clones examined. Details for the generation of transgenic flies, MARCM clone induction, immunohistochemistry of fly brains, image processing and quantification methods are available upon request.

**Table S1. Whole Exome Sequence Output and Coverage for Coding Sequences**

| <b>Family ID</b> | <b>Individual ID</b> | <b>Identification</b> | <b>Capture</b> | <b>Total (bps)</b> | <b>Mean depth</b> | <b>% ≥ 5×</b> | <b>% ≥ 10×</b> | <b>% ≥ 20×</b> |
|------------------|----------------------|-----------------------|----------------|--------------------|-------------------|---------------|----------------|----------------|
| <b>Family 1</b>  | I-1                  | Father                | V5             | 3,199,010,619      | 95.57             | 97.2          | 96.2           | 93.1           |
| <b>Family 1</b>  | I-2                  | Mother                | V5             | 2,902,625,566      | 86.72             | 97            | 95.8           | 92.2           |
| <b>Family 1</b>  | II-2                 | Affected individual   | V5             | 3,766,100,939      | 112.51            | 97.3          | 96.4           | 93.7           |
| <b>Family 2</b>  | I-1                  | Father                | V5             | 4,609,239,531      | 137.7             | 97.4          | 96.8           | 95.1           |
| <b>Family 2</b>  | I-2                  | Mother                | V5             | 4,259,106,595      | 127.24            | 97.4          | 96.7           | 94.9           |
| <b>Family 2</b>  | II-1                 | Affected individual   | V5             | 2,914,949,565      | 87.09             | 97            | 95.9           | 92.4           |
| <b>Family 3</b>  | II-1                 | Affected individual   | V4             | 4,022,246,545      | 120.17            | 96.2          | 95.2           | 92.9           |
| <b>Family 4</b>  | II-1                 | Affected individual   | V5             | 2,939,319,692      | 87.81             | 97.1          | 96             | 92.7           |

**Table S2. Priority Scheme of Homozygous Variants in Four Families**

|  | <b>Family 1</b> | <b>Family 2</b> | <b>Family 3</b> | <b>Family 4</b> |
|--|-----------------|-----------------|-----------------|-----------------|
| <b>Homozygous in affected person as autosome*</b>                | 2233            | 2219            | 2111            | 2094            |
| <b>Non-homozygous in father</b>                                  | 378             | 400             | NA              | NA              |
| <b>Non-homozygous in mother</b>                                  | 159             | 193             | NA              | NA              |
| <b>Frequency of <math>\leq 0.005</math> in ExAC</b>              | 38              | 42              | 164             | 152             |
| <b>Frequency of <math>\leq 0.005</math> in EVS</b>               | 35              | 39              | 141             | 136             |
| <b>Frequency of <math>\leq 0.005</math> in HGVD</b>              | 22              | 25              | 114             | 118             |
| <b>Frequency of <math>\leq 5/575</math> in in-house database</b> | 3               | 4               | 1               | 33              |
| <b>Non-synonymous</b>  | 3               | 3               | 1               | 25              |

NA: not analyzed by WES, ExAC: Exome Aggregation Consortium, EVS: Exome Variant Server, HGVD: Human Genetic Variation Database. \*The number of the variants in exons and  $\pm$  intronic 30 bp regions from exon–intron borders.

**Table S3. Priority Scheme of Compound Heterozygous Variants in Four Families**

|  | <b>Family 1</b> | <b>Family 2</b> | <b>Family 3</b> | <b>Family 4</b> |
|--|-----------------|-----------------|-----------------|-----------------|
| <b>Heterozygous variants in affected person as autosome</b>      | 4060            | 4073            | 3871            | 3676            |
| <b>Non-homozygous in father</b>                                  | 3737            | 3719            | NA              | NA              |
| <b>Non-homozygous in mother</b>                                  | 3412            | 3384            | NA              | NA              |
| <b>Frequency of <math>\leq 0.005</math> in ExAC</b>              | 1727            | 1778            | 1828            | 1341            |
| <b>Frequency of <math>\leq 0.005</math> in EVS</b>               | 1698            | 1748            | 1790            | 1254            |
| <b>Frequency of <math>\leq 0.005</math> in HGVD</b>              | 1100            | 1101            | 1376            | 1210            |
| <b>Frequency of <math>\leq 5/575</math> in in-house database</b> | 578             | 534             | 889             | 918             |
| <b>Non-synonymous</b>  | 421             | 401             | 664             | 667             |
| <b>Two or more variants in one gene</b>                          | 36              | 38              | 91              | 78              |
| <b>Compound heterozygous variant (gene)</b>                      | 14 (6)          | 19 (8)          | ND              | ND              |

NA: not analyzed by WES, ND: not determined, ExAC: Exome Aggregation Consortium, EVS: Exome Variant Server, HGVD: Human Genetic Variation Database.

**Table S4. Clinical comparison between *TBCD* and *TBCE* mutations**

|                              | <i>TBCD</i> mutation<br>(number in our cohort) |             | <i>TBCE</i> mutation <sup>a</sup> |
|------------------------------|--|-------------|-----------------------------------|
| Onset age                    | < 11 months                                    |             | < 7 months                        |
| Intellectual disability      | +  | (8/8, 100%) | +                                 |
| Microcephaly                 | +  | (8/8, 100%) | +                                 |
| Muscle weakness              | +  | (7/7, 100%) | Not mentioned                     |
| Regression                   | +  | (6/6, 100%) | Not mentioned                     |
| Muscle atrophy               | +  | (6/8, 75%)  | Not mentioned                     |
| Postnatal growth retardation | +  | (6/8, 75%)  | +                                 |
| Seizure                      | +  | (6/8, 75%)  | - <sup>b</sup>                    |
| Respiratory failure          | +  | (5/8, 63%)  | -                                 |
| Optic nerve atrophy          | +  | (4/8, 50%)  | Not mentioned                     |
| Bone abnormality             | Bone fractures                                 | (2/8, 25%)  | Bone dysplasia [KCS]              |
| Hypoparathyroidism           | -  |             | +                                 |
| Recurrent infection          | -  |             | + [KCS]                           |
| IUGR                         | -  |             | +                                 |
| Facial dysmorphism           | -  |             | +                                 |
| Deep set eyes                | -  |             | +                                 |
| Thin lips                    | -  |             | +                                 |
| Beaked nose tip              | -  |             | +                                 |
| Depressed nasal bridge       | -  |             | +                                 |
| External ear anomalies       | -  |             | +                                 |
| Micrognathia                 | +  |             | +                                 |
| Brain MRI findings           |  |             |                                   |
| Hypoplastic corpus callosum  | +  |             | +                                 |
| Decreased white matter       | +  |             | +                                 |

<sup>a</sup>The clinical information of *TBCE* mutation was based on papers by Sanjad et al. (1991) and Padidela et al. (2009).<sup>9,10</sup> <sup>b</sup>Only one affected individual showed seizures but with hypocalcemia.<sup>10</sup> [KCS]: The feature was only reported in Kenny-Caffey syndrome with *TBCE* mutations.

**Table S5. Internal organ involvement in autopsied Individual 1**

| Organs           | Findings   |
|------------------|--|
| Heart            | Normal shape. Normal cardiac muscle development.   |
| Lung             | Left: Lower lobe was atelectatic and shrunk.<br>Right: Upper and middle lobes were atelectatic and shrunk. |
| Thymus           | Prominent calcification was observed in Hassall's corpuscles.  |
| Thyroid          | Not examined.  |
| Parathyroid      | Not examined.  |
| Digestive tracts | No structural abnormality.   |
| Liver            | Fatty liver appearance.  |
| Gallbladder      | No remarkable change.  |
| Adrenal glands   | No remarkable change.  |
| Spleen           | No remarkable change.  |
| Kidney           | No remarkable change.  |
| Urinary tracts   | No remarkable change.  |
| Urinary bladder  | No remarkable change.  |
| Uterus           | No remarkable change.  |
| Ovary            | Multiple follicular cysts in both ovaries.   |

**Table S6. Possible genotype–phenotype correlation between mutation and clinical severity**

|                        | <b>Family 1</b>   |             | <b>Family 2</b> |              | <b>Family 3</b> |              | <b>Family 4</b>  |
|------------------------|-------------------|-------------|-----------------|--------------|-----------------|--------------|------------------|
| Clinical severity      | Profound          |             | Severe          |              | Severe          |              | Mild             |
| Mutation               | c.1564-12C>G      | c.2314C>T   | c.1160T>G       | c.2761G>A    | c.2280C>A       | c.3365C>T    | c.2810C>G (homo) |
| Amino acid             | p. Gly522Phefs*14 | p.Arg772Cys | p.Met387Arg     | p. Ala921Thr | p.Tyr760*       | p.Pro1122Leu | p.Pro937Arg      |
| Type                   | frameshift        | missense    | missense        | missense     | nonsense        | missense     | missense         |
| Binding with ARL2      | NA                | ↓           | ↓↓              | ↓            | ↓               | ↓            | →                |
| Binding with TBCE      | NA                | ↓           | ↓↓              | ↓↓           | ↓↓              | ↓↓           | ↓                |
| Binding with β-tubulin | NA                | ↓↓          | ↓↓              | ↓↓           | ↓↓              | ↓↓           | ↓                |

NA: not assessed as TBCD protein may not exist due to NMD.

## Supplemental References

1. Kelley, L.A., Mezulis, S., Yates, C.M., Wass, M.N., Sternberg, M.J. (2015). The Phyre2 web portal for protein modeling, prediction and analysis. *Nat Protoc* 10, 845-858.
2. Kobayashi, J., Matsuura, Y. (2013). Structural basis for cell-cycle-dependent nuclear import mediated by the karyopherin Kap121p. *J Mol Biol* 425, 1852-1868.
3. Fournier, D., Palidwor, G.A., Shcherbinin, S., Szengel, A., Schaefer, M.H., Perez-Iratxeta, C., Andrade-Navarro, M.A. (2013). Functional and genomic analyses of alpha-solenoid proteins. *PLoS One* 8, e79894.
4. Nithianantham, S., Le, S., Seto, E., Jia, W., Leary, J., Corbett, K.D., Moore, J.K., Al-Bassam, J. (2015). Tubulin cofactors and Arl2 are cage-like chaperones that regulate the soluble alphabeta-tubulin pool for microtubule dynamics. *Elife* 4.
5. Pettersen, E.F., Goddard, T.D., Huang, C.C., Couch, G.S., Greenblatt, D.M., Meng, E.C., Ferrin, T.E. (2004). UCSF Chimera--a visualization system for exploratory research and analysis. *J Comput Chem* 25, 1605-1612.
6. Cook, A., Fernandez, E., Lindner, D., Ebert, J., Schlenstedt, G., Conti, E. (2005). The structure of the nuclear export receptor Cse1 in its cytosolic state reveals a closed conformation incompatible with cargo binding. *Mol Cell* 18, 355-367.

7. Hanzal-Bayer, M., Renault, L., Roversi, P., Wittinghofer, A., Hillig, R.C. (2002). The complex of Arl2-GTP and PDE delta: from structure to function. *EMBO J* 21, 2095-2106.
8. Lowe, J., Li, H., Downing, K.H., Nogales, E. (2001). Refined structure of alpha beta-tubulin at 3.5 A resolution. *J Mol Biol* 313, 1045-1057.
9. Sanjad, S.A., Sakati, N.A., Abu-Osba, Y.K., Kaddoura, R., Milner, R.D. (1991). A new syndrome of congenital hypoparathyroidism, severe growth failure, and dysmorphic features. *Arch Dis Child* 66, 193-196.
10. Padidela, R., Kelberman, D., Press, M., Al-Khawari, M., Hindmarsh, P.C., Dattani, M.T. (2009). Mutation in the TBCE gene is associated with hypoparathyroidism-retardation-dysmorphism syndrome featuring pituitary hormone deficiencies and hypoplasia of the anterior pituitary and the corpus callosum. *J Clin Endocrinol Metab* 94, 2686-2691.